REDVET - Revista electrónica de Veterinaria - ISSN 1695-7504
Vol 25, No. 1 (2024)
http://www.veterinaria.org
Article Received: 21/04/2023 Revised: 12/05/2023 Accepted: 01/06/2024

Thermal decomposition of 3-butyl-2,6-bis(4-fluorophenyl)piperidin-4-one in nitrogen atmosphere-Non-isothermal condition

G.Vallal Perumal[1], V.J.Ramya Devi[2], G.Rajarajan[3,4,*] and V.Thanikachalam[5]

[1,2, 3,5]Department of Chemistry, Annamalai University, Annamalainagar-608002, India;
[4*]Department of Chemistry, Bharathiar University, Coimbatore-641046, India

***Corresponding Author:** Dr. G.Rajarajan, Ph. D.,
Associate Professor, Department of Chemistry, Annamalai University, Annamalainagar-608002, Tamil Nadu, India.
Tel:9080962750. E-mail address: rajarajang70@gmail.com.

ABSTRACT
The compound 3-butyl-2,6-bis(4-fluorophenyl)piperidin-4-one was synthesized by refluxed with ammonium acetate, 2-heptanone and 4-flurobenzaldehyde using distilled ethanol. The synthesized product was characterized using FT-IR and NMR spectroscopy. Its thermal behavior was examined through decomposition studies carried out with a system integrating thermogravimetric analysis (TG), differential thermal analysis (DTA) and differential thermogravimetric analysis (DTG) under a dynamic nitrogen atmosphere over a range of temperatures. Kinetic and thermodynamic parameters were determined using iso-conversional model-free approaches, including the Friedman, Flynn-Wall-Ozawa (FWO) and Kissinger-Akahira-Sunose (KAS) methods. For model-fitting analysis, the Coats-Redfern method was employed. The TG curves revealed a single-step decomposition process. Activation energy (E_a) values and correlation coefficients (r) were obtained and graphically represented based on the isoconversional methods. Comparison of the theoretical reaction models with experimental results indicated that the compound decomposes according to a third order mechanism (F3 model).

Keywords: TG, DTA, DTG, Friedmann, KAS, FWO, model fitting analysis and F3 model.

1. Introduction

Heterocyclic compounds are essential participants in numerous biochemical processes within the human body, making them vital frameworks in medicinal chemistry for designing diverse therapeutic agents. Among these heterocyclic structures containing both nitrogen and oxygen atoms have gained significant interest from synthetic chemists because of their wide range of biological activities [1] such as local anesthetic [2,3], bactericidal, fungicidal and depressant drugs [4,5]. Nitrogen-containing heterocycles, particularly piperidines, represent an important class of compounds in medicinal chemistry, as piperidin-4-one moieties are found in numerous naturally occurring alkaloids. Moreover, piperidines have extensive pharmaceutical applications and are key structural units in various drugs such as paroxetine, raloxifene, haloperidol, droperidol and minoxidil [6-8]. The nitrogen atom of the C=N group acts as an excellent electron donor, and when combined with additional oxygen or nitrogen donor atoms at the coordination sites, the resulting compounds function as highly effective polydentate ligands for transition metal complexes [9]. Piperidine scaffolds featuring cis-substituents at the 2- and 6-positions and a carbonyl or hydroxyl group at the 4-position are of particular interest. Consequently, the asymmetric synthesis of these polysubstituted piperidine derivatives has attracted considerable attention, prompting the development of numerous strategies for their efficient preparation [10-16]. Piperidines can be substituted at all six positions of the heterocyclic ring, resulting in a diverse array of derivatives. Early investigations suggest that piperidin-2-one derivatives are promising candidates for the development of c-Met protein inhibitors targeting lung cancer, as well as for therapeutic interventions in Alzheimer's disease [17,18]. Aromatic aldehydes can act as key precursors for the formation of piperidine rings, facilitating the synthesis of 4-phenylpiperidine derivatives. Ammonium acetate serves as an accessible and economical reagent for the preparation of nitrogen-containing compounds[19]. The diverse biological activities exhibited by THPs and piperidin-4-ones, along with their significant involvement in various disease processes, have motivated investigations into their potential applications in agrochemicals and pharmaceuticals. Several synthetic approaches have been reported for these compounds, including imino-Diels-Alder reactions, aza-Prins cyclizations, intramolecular Michael reactions and intramolecular Mannich reactions [20-25] involving iminium ions, among others. A novel set of piperidin-4-one derivatives was synthesized to investigate their stereochemical influence[26]. The therapeutic potential of piperidin-4-one analogues largely depends on their molecular sensitivity and ring conformations with particular emphasis on 2,6-disubstituted derivatives. While they are known to display UV absorption, the restricted nature of the absorption spectrum highlights the need to investigate the structural factors governing these properties[27-35]. The symmetric compound 3,5-bis(2-fluorobenzylidene)-4-piperidone (EF24) exhibits strong antitumor activity, suppressing tumor progression and metastasis through the inhibition of NF-κB-dependent signaling pathways [36]. Detailed investigations have been carried out on the *in vitro* growth inhibition and apoptosis induction in the human laryngeal epithelial cancer cell line (HEp-2) by 3-methyl-2,6-bis(4-tolyl) piperidin-4-one and its N(4')-cyclohexylsemicarbazone [37]. Although

both experimental and computational studies have been carried out on the biological activities of halogen-substituted 4-piperidone curcumin analogs, the available theoretical and quantum chemical investigations on these compounds remain limited. Prior work has examined the HOMO–LUMO energies, Fukui and Parr functions, and electron affinities of N-methyl-4-piperidone and N-benzyl-4-piperidone curcumin analogs, including their radical anions. These studies evaluated the influence of different aromatic substituents on the electronic properties and concluded that substitution at the nitrogen atom (methyl or benzyl) does not significantly alter the frontier molecular orbitals, whereas substituents on the phenyl ring play a more dominant role. However, the reported calculations were restricted to *para*-chloro- and *para*-bromo-substituted N-methyl-4-piperidone derivatives. Comprehensive analyses involving electron density mapping, spectroscopic behavior, bonding characteristics, and nonlinear optical properties of these analogs are still lacking. Theoretical modeling is crucial, as it provides a molecular-level understanding of structure-property relationships and can be used to predict physicochemical properties prior to synthesis [38,39]. The present article reports the thermal degradation of synthesised compound under non-isothermal condition.

2. Materials and Methods

2.1 Experimental characterizations

All syntheses were carried out using high-purity annular-grade reagents such as 4-flurobenzaldehyde, 2-heptanone, ammonium acetate, distilled ethanol and ammonia. Melting points were measured in open capillaries. Reaction progress was monitored by thin-layer chromatography (TLC) on Merck silica gel 60 F254 pre-coated aluminum plates, using petroleum ether and ethyl acetate as the mobile phase. Infrared spectra were recorded on an AVATAR-330 FT-IR spectrometer (Thermo-Nicolet). Proton (^{1}H) and carbon (^{13}C) NMR spectra were obtained on Bruker instruments operating at 400 MHz and 100 MHz, respectively, with tetramethylsilane (TMS) as an internal reference and chemical shifts reported in δ (ppm). Thermal studies were carried out using a simultaneous thermogravimetric and differential thermal analyzer (STA 7200, Hitachi HTG, Japan) at Vignan University, Vadlamudi, Andhra Pradesh. Thermogravimetric (TG), differential thermal (DTA), and derivative thermogravimetric (DTG) analyses were conducted in ceramic crucibles under static nitrogen gas with a flow rate of 100 mL/min. Approximately 8 mg of sample was heated from 23 to 830°C at heating rates of 10, 15 and 20 °C/min. The sample temperature was controlled by a thermocouple, ensuring accurate tracking of the programmed heating profile. Kinetic parameters including activation energy (E_a) and the logarithmic pre-exponential factor (ln A) were calculated using dedicated software.

2.2 General Procedure

Synthesis of 3-butyl-2,6-bis(4-fluorophenyl)piperidin-4-one)

The target compound was synthesized following a reported procedure [40] for 2,6-diarylpiperidin-4-ones. A reaction mixture containing ammonium acetate (0.05 mol), 4-fluorobenzaldehyde (0.1 mol) and 2-heptanone (0.05 mol) in distilled ethanol was heated to reflux. Upon cooling, the resulting viscous mass was dissolved in ether (200 mL) and treated with concentrated hydrochloric acid (10 mL). The precipitated hydrochloride of 3-butyl-2,6-bis(4-fluorophenyl)piperidin-4-one was collected by filtration and sequentially washed with ethanol-ether (1:1) followed by ether to remove colored impurities. The free base was obtained by treating the alcoholic solution with aqueous ammonia and subsequently diluting with water. The final product was purified by recrystallization from ethanol**.** Yield 85%; m.p.: 85(ºC); MF: $C_{21}H_{23}NF_2$; IR (KBr) (cm^{-1}): 3287 (N-H stretching), 2922 (aliphatic CH stretching), 1714 (C=O stretching), 1513 (C=C stretching), 1088 (C-N stretching), 820 (aromatic C-H out of plane bending vibration); ^{1}H NMR (400 MHz, $CDCl_3$, δ,ppm): 6.99-7.45 (m, 8H, Ar-H), 4.07 (d,1H, H6) , 3.72 (d, 1H, H2), 2.56-2.63 (2H, H3a,H5eq), 1.59 (1H, H5ax), 0.96-1.25 (m, 6H, CH_2), 0.74 (t, 3H, CH_3); ^{13}C NMR (100 MHz, CDCl3, δ, ppm): 208.76 C(4), 115.13-138.53 (Ar-C), 66.34 C(2), 61.08 C(6), 51.62 C(3), 38.63 C(5), 22.75-29.89(CH_2), 13.80 (CH_3) in the **Fig.1.**

REDVET - Revista electrónica de Veterinaria - ISSN 1695-7504
Vol 25, No. 1 (2024)
http://www.veterinaria.org
Article Received: 21/04/2023 Revised: 12/05/2023 Accepted: 01/06/2024

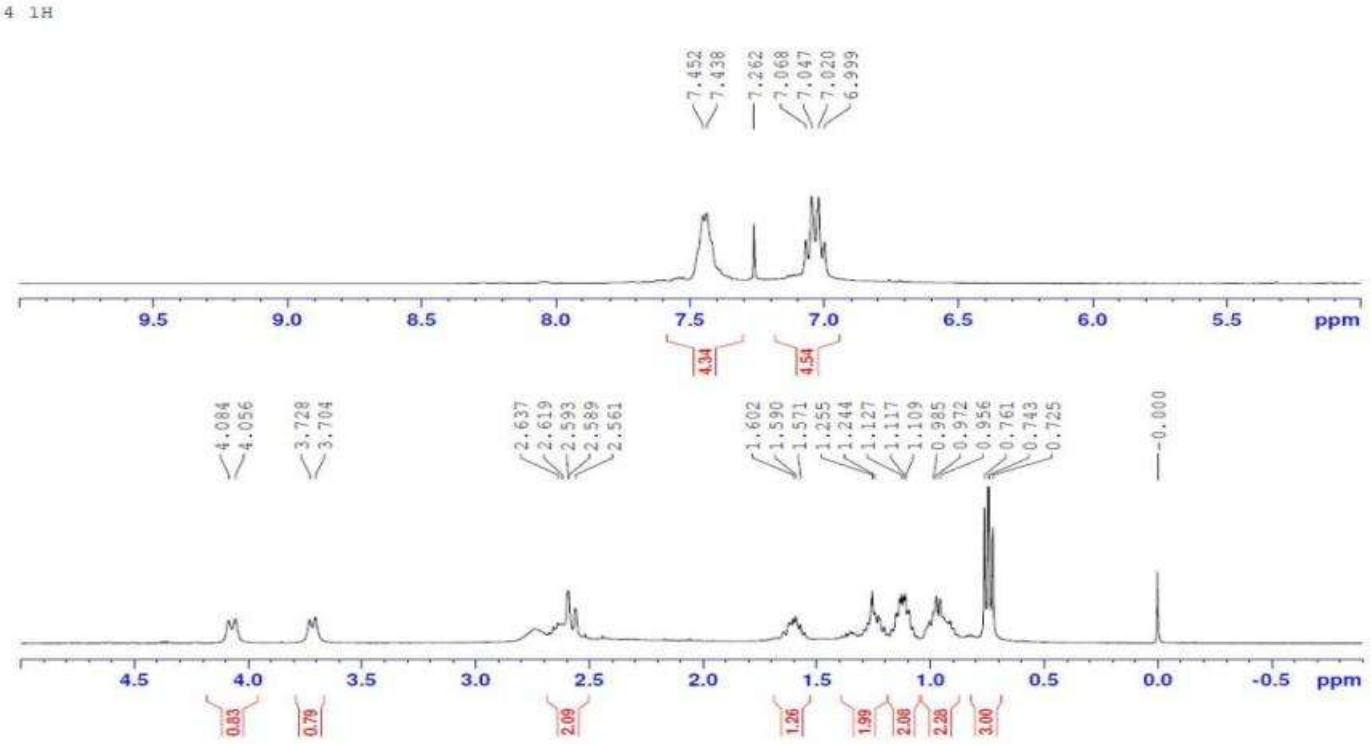

REDVET - Revista electrónica de Veterinaria - ISSN 1695-7504
Vol 25, No. 1 (2024)
http://www.veterinaria.org
Article Received: 21/04/2023 Revised: 12/05/2023 Accepted: 01/06/2024

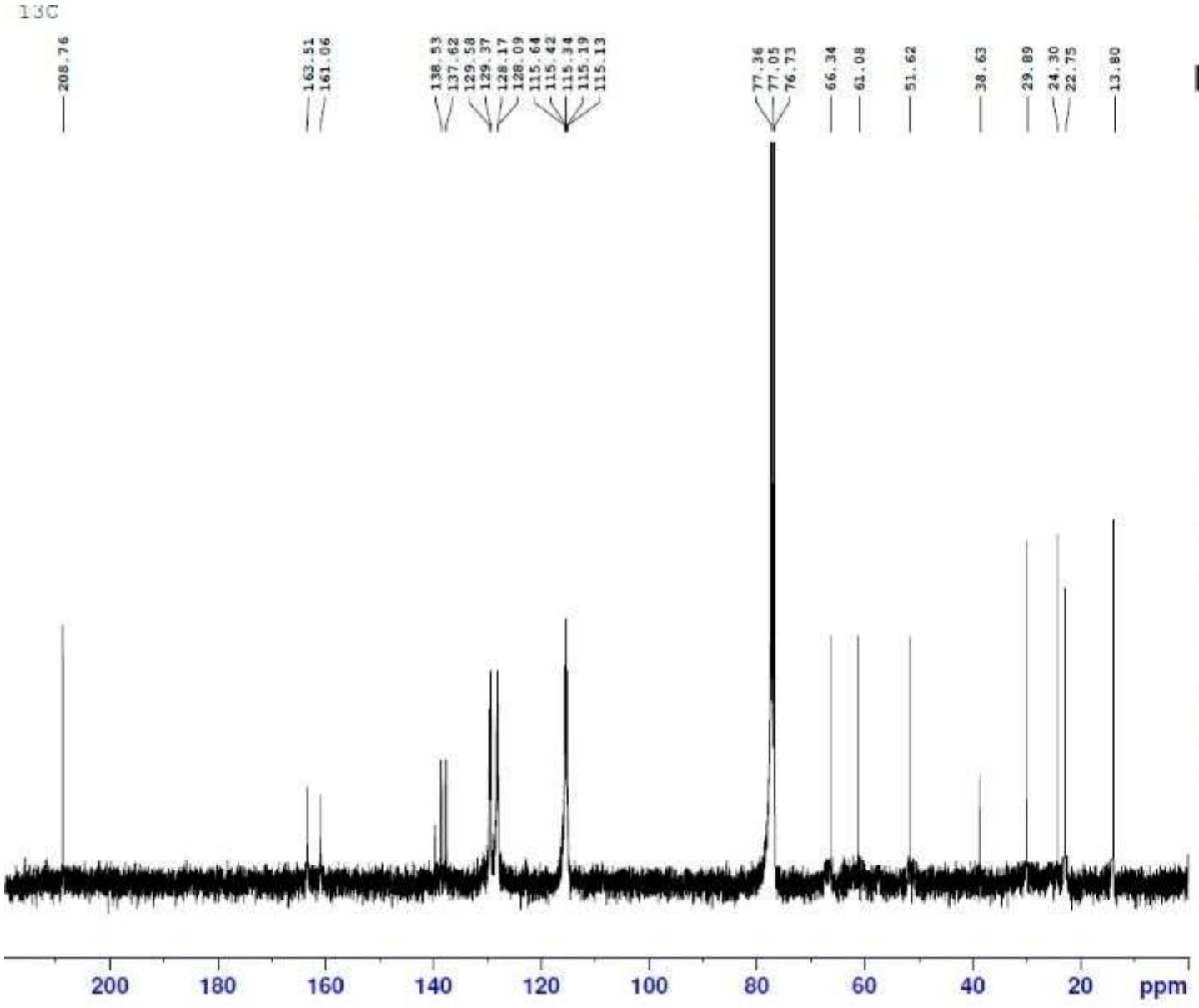

Fig 1. ^{1}H and ^{13}C NMR spectra of BFPPO in $CDCl_3$ medium

2.3 Thermal analysis

In thermogravimetric analysis, the conversion (α) is expressed as the fraction of mass lost at a specific stage relative to the total mass loss observed for the complete decomposition process. The Friedman [41] isoconversional (model-free) approach is employed to evaluate how the activation energy (Ea) varies with the degree of conversion (α). The Flynn-Wall-Ozawa (FWO) [42] method is a model-free approach in which ln β is plotted against 1/T. The activation energy (Ea) is then determined from the slope of these plots, using temperatures corresponding to fixed conversion levels obtained from experiments conducted at different heating rates (β).The Kissinger-Akahira-Sunose (KAS)[43] method is a kinetic analysis technique used to relate the activation energy to the degree of conversion in dynamic studies conducted at different constant heating rates. By plotting $\ln(\beta/T^2)$ against 1/T at appropriate conversion levels, a linear relationship is obtained, from which the slope and intercept are used to calculate the activation energy and pre-exponential (frequency) factor. Kinetic parameters were determined using approximately fifteen models within the

REDVET - Revista electrónica de Veterinaria - ISSN 1695-7504
Vol 25, No. 1 (2024)
http://www.veterinaria.org
Article Received: 21/04/2023 Revised: 12/05/2023 Accepted: 01/06/2024

Coats-Redfern framework. The model exhibiting the highest linearity was chosen for analysis. From the resulting linear plot of $\ln[g(\alpha)/T^2]$ versus 1/T, the activation energy and pre-exponential factor were obtained from the slope and intercept, respectively. The pre-exponential (frequency) factor and thermodynamic parameters including the enthalpy of activation ($\Delta H^{\neq}$), entropy of activation ($\Delta S^{\neq}$), and Gibbs free energy of activation ($\Delta G^{\neq}$) were calculated[414].

3. Results and discussion

The Thermogravimetric (TG) analysis performed at heating rates of 10, 15 and 20 °C min^{-1} **(Fig. 2a-c)** demonstrates that the compound decomposes through a single-step process. According to the TG results, melting initiates at 195°C, while thermal degradation begins around 200 °C. The major weight loss is observed from room temperature up to 200°C and continues until approximately 421°C. Furthermore, an increase in heating rate leads to a noticeable shift of the maximum decomposition temperature toward higher values, as imitated in the asymmetric TG frameworks.The compound's thermal behavior was examined through non-isothermal decomposition using model-free kinetic approaches such as the Friedman[41], Flynn-Wall-Ozawa (FWO)[42], and Kissinger-Akahira-Sunose (KAS)[43] methods. Analysis of the data highlights changes in the apparent activation energy (E_a) as a function of the conversion degree (α). Across the conversion interval of 0.20 to 0.90, E_a shows a slight deterioration at first, followed by an increase with further conversion Table 1. The E_a values obtained through the Friedman and FWO isoconversional techniques are in good agreement. These findings suggest that the apparent activation energy is conversion-dependent, offering deeper insight into the complex decomposition pathway and helping in elucidating its mechanism. Using the Friedman approach, the mean activation energy for decomposition within the 0.10 to 0.90 conversion range was calculated as 107.34±3.4 kJ mol^{-1}. The activation energies derived from this method closely align with those determined by FWO and show consistency with KAS results. Within the same interval, Ea values remain relatively stable regardless of the method applied, with averages of 107.34±3.4, 100.98 ±3.3 and 105.00 ±3.3 kJ mol^{-1} for Friedman, KAS and FWO methods, respectively.

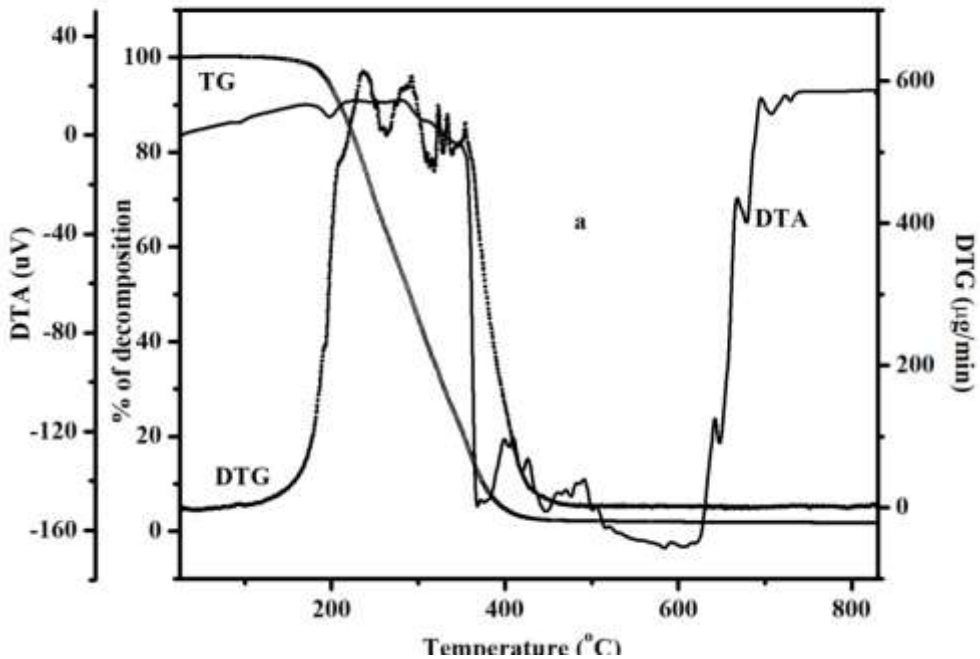

REDVET - Revista electrónica de Veterinaria - ISSN 1695-7504
Vol 25, No. 1 (2024)
http://www.veterinaria.org
Article Received: 21/04/2023 Revised: 12/05/2023 Accepted: 01/06/2024

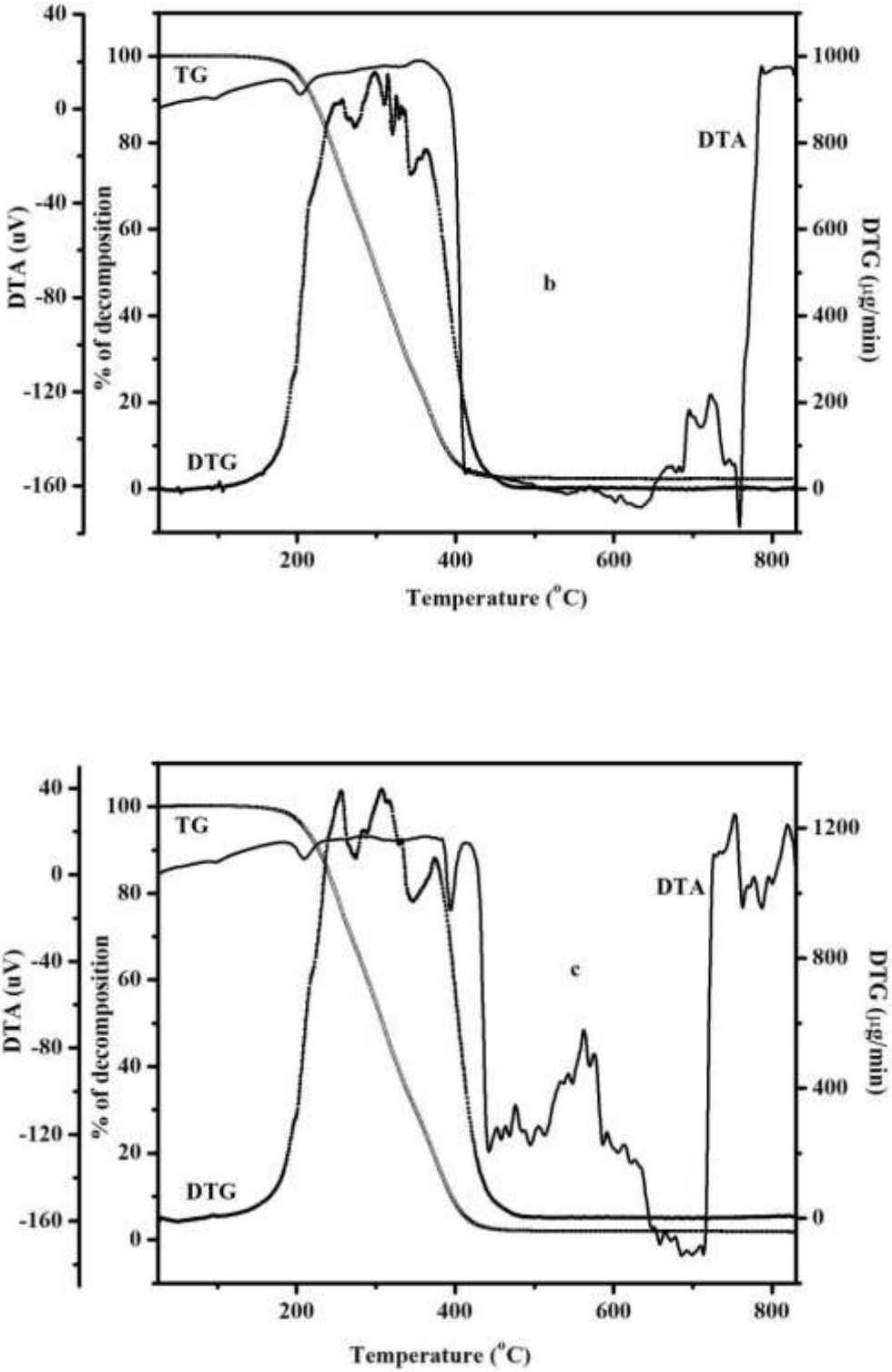

Fig 2. TGA, DTG and DTA curves of BFPPO at heating rates a) 10°C , b)15°C and c)20°C/min in nitrogen atmosphere

Table 1. Temperatures corresponding to the same degree of conversion at different heating rates for BFPPO

α	Temperature (K)	Friedman method	KAS method	FWO method

REDVET - Revista electrónica de Veterinaria - ISSN 1695-7504
Vol 25, No. 1 (2024)
http://www.veterinaria.org
Article Received: 21/04/2023 Revised: 12/05/2023 Accepted: 01/06/2024

	10 (°C/min)	15 (°C/min)	20 (°C/min)	E_a (kJ mol^{-1})	r	E_a (kJ mol^{-1})	r	E_a (kJ mol^{-1})	r
0.05	468.93	476.14	483.75			80.23	-0.993	83.82	-0.995
0.1	483.63	491.48	499.13	83.97	-0.999	81.70	-0.996	85.46	-0.997
0.15	495.18	503.05	511.02	88.27	-0.993	83.74	-0.995	87.59	-0.996
0.20	505.29	513.14	520.99	98.64	-0.997	88.17	-0.995	91.96	-0.996
0.25	514.92	523.21	531.30	86.88	-0.997	87.68	-0.996	91.65	-0.997
0.30	523.84	532.20	540.37	96.44	-0.996	89.97	-0.996	93.97	-0.997
0.35	533.09	541.23	549.27	110.21	-0.996	95.40	-0.996	99.28	-0.996
0.40	543.55	551.60	560.00	102.66	-0.990	97.42	-0.994	101.36	-0.995
0.45	553.68	562.10	570.37	105.43	-0.999	99.83	-0.996	103.81	-0.996
0.50	563.99	572.30	581.00	106.04	-0.989	101.44	-0.994	105.52	-0.995
0.55	573.66	582.23	590.80	111.81	-0.998	104.36	-0.995	108.44	-0.996
0.60	583.21	591.70	600.66	110.24	-0.989	105.76	-0.993	109.93	-0.995
0.65	593.84	602.62	611.41	117.21	-0.999	109.16	-0.995	113.33	-0.996
0.70	604.04	612.89	621.74	120.13	-0.996	112.18	-0.995	116.36	-0.996
0.75	615.16	624.08	632.98	124.07	-0.996	115.65	-0.995	119.84	-0.996
0.80	626.85	636.00	644.70	130.12	-0.999	120.13	-0.997	124.28	-0.997
0.85	636.81	645.00	654.94	127.33	-0.989	121.87	-0.995	126.11	-0.996
0.90	649.16	658.30	667.80	126.16	-0.993	123.04	-0.994	127.41	-0.995
				107.34±3.4		100.98 ±3.3		105.00 ±3.3	

3.1 Model-fitting analysis

All 15 kinetic models[45] listed in Table 2 were applied to the non-isothermal data of the compound over the conversion interval $0.10 \leq \alpha \leq 0.90$, where the model-free approach indicated nearly constant activation energy. The selection of a specific reaction model strongly influences the evaluated kinetic parameters, including activation energy (E_a), pre-exponential factor (ln A), correlation coefficient (r), and the mechanistic interpretation of the decomposition process. Furthermore, the invariant kinetic parameters method supports these results, verifying that the compound undergoes decomposition through a single-step mechanism.

Table 2. Determination of apparent activation parameters by Coats-Redfern method for each heating rate of BFPPO in the nitrogen atmosphere

Kinetic model	β = 10 °C/min			β = 15 °C/min			β = 20 °C/min		
	E_a (kJ mol^{-1})	ln *A* (A/min)	r	E_a (kJ mol^{-1})	ln *A* (A/min)	r	E_a (kJ mol^{-1})	ln *A* (A/min)	r
P2	7.96	-2.57	-0.816	8.20	-2.10	-0.843	8.43	-1.76	-0.859
P3	1.22	-5.43	-0.356	1.39	-4.88	-0.417	1.51	-4.50	-0.458
P4	-1.44		0.502	-1.33		0.490	-1.25		0.481
F1	35.52	5.01	-0.976	36.49	5.57	-0.985	37.22	5.96	-0.991
F2	53.52	9.70	-0.980	54.90	10.32	-0.988	55.96	10.75	-0.993

REDVET - Revista electrónica de Veterinaria - ISSN 1695-7504
Vol 25, No. 1 (2024)
http://www.veterinaria.org
Article Received: 21/04/2023 Revised: 12/05/2023 Accepted: 01/06/2024

F3	75.80	15.31	-0.969	77.69	16.00	-0.977	79.16	16.48	-0.981
D1	64.14	17.98	-0.963	65.64	18.62	-0.969	66.81	19.07	-0.973
D2	61.68	9.39	-0.964	63.24	10.03	-0.972	64.45	10.48	-0.976
D3	70.74	10.20	-0.975	72.51	10.87	-0.982	73.88	11.34	-0.987
D4	64.66	8.65	-0.968	66.29	9.31	-0.976	67.55	9.76	-0.980
A2	13.05	-0.51	-0.954	13.49	-0.01	-0.971	13.82	0.33	-0.981
A3	5.54	-2.88	-0.893	5.81	-2.39	-0.930	6.01	-2.05	-0.953
A4	1.81	-4.75	-0.644	1.99	-4.22	-0.744	2.12	-3.86	-0.813
R2	28.42	2.39	-0.959	29.22	2.93	-0.969	29.83	3.30	-0.975
R3	26.41	2.11	-0.951	27.17	2.64	-0.961	27.74	3.01	-0.968

3.2 Invariant kinetic models

The invariant kinetic parameter method was applied to data obtained at heating rates of 10, 15, and 20 °C min^{-1}. Kinetic parameters were calculated using the Coats–Redfern method, and the results are summarized in Table 3. For all examined models, the Coats-Redfern[45] plots produced nearly linear relationships with correlation coefficients close to unity over the conversion range of $0.10 \leq \alpha \leq 0.90$. As shown in Table 3, both the activation energy (Ea) and pre-exponential factor (ln A) are influenced by the heating rate as well as the selected model. The invariant kinetic parameters, defined as ln A_{inv} and E_{inv}, were obtained by plotting ln A_{inv} against E_{inv} across different heating rates, where the resulting lines intersected at a characteristic point (E_{inv}, A_{inv})[46-48]. These values were further evaluated using the supercorrelation equation. In this approach, a plot of a_β versus b_β at three heating rates yielded a straight line, from which ln A_{inv} and E_{inv} were derived. Among the tested models, the third order model showed the best agreement, with its apparent parameters supported by high correlation coefficients (Table 4).

Table 3. Compensation effect parameters for several combinations of kinetic models for BFPPO in the nitrogen atmosphere

β (°C /min)	AKM			AKM-D1,D2}		
	a_β (*A*/min)	b_β (mol J^{-1})	r	a_β (*A*/min)	b_β (mol J^{-1})	r
10	0.23646	-4.47742	0.981	0.23646	-4.47742	0.980
15	0.23354	-4.01964	0.981	0.23354	-4.01964	0.981
20	0.23112	-3.70312	0.982	0.23112	-3.70312	0.982
β (°C /min)	**AKM-P2-P4,D1-D4}**			**AKM-P2-P4, F2,F3,D1-D4, R3}**		
	a_β (*A*/min)	b_β (mol J^{-1})	r	a_β (*A*/min)	b_β (mol J^{-1})	r
10	0.26462	-4.64351	0.997	0.26672	-4.64647	0.990
15	0.26122	-4.20228	0.998	0.26237	-4.19044	0.991
20	0.2584	-3.89477	0.998	0.25899	-3.87372	0.992

Table 4. Isokinetic parameters of kinetic models for BFPPO in the nitrogen atmosphere.

Kinetic model	E_{inv}(kJ mol^{-1})	ln A_{inv}(A/min)	-r
AKM	127.82	27.80	-0.999
AKM-D1,D2}	145.40	29.91	-0.998
AKM-P2-P4,D1-D4}	120.69	27.30	-0.999
AKM-P2-P4, F2,F3,D1-D4, R3}	100.19	22.08	-0.999

3.3 Determination of the kinetic model by master plots

The integral form of the conversion function for solid-state non-isothermal decomposition reactions [49] is expressed as:

$$g(\alpha) = \frac{A}{\beta}\int_{T_0}^{T} \exp\left(-\frac{E_a}{RT}\right)dT = \frac{AE_a}{R\beta}p(u) \qquad \text{.....(1)}$$

where $p(u) = \int_{\infty}^{u} \frac{exp(-u)}{u^2}du$

$u=E_a/RT$

Taking $\alpha = 0.5$ as the reference point, the FWO method yields the following expression.

REDVET - Revista electrónica de Veterinaria - ISSN 1695-7504
Vol 25, No. 1 (2024)
http://www.veterinaria.org
Article Received: 21/04/2023 Revised: 12/05/2023 Accepted: 01/06/2024

$$g(\alpha_{0.5}) = (\frac{AE}{\beta R})p(u_{0.5}) \quad \text{.....(2)}$$

The plots of $g(\alpha)/g(\alpha_{0.5})$ versus α show good agreement with the theoretical master plots of several hypothetical g(α) functions presented in Table 4. An accurate expression [49] was employed to construct the experimental master plots of $p(u)/p(u_{0.5})$ from data obtained at different heating rates:

$$p(u) = \exp(-u) / [u(1.00198882u + 1.87391198)] \quad \text{....(3)}$$

According to Eq. (3), when the appropriate kinetic model is applied, the experimental values of $g(\alpha)/g(\alpha_{0.5})$ remain consistent for a given α. Thus, the kinetic model can be identified by comparing experimental and theoretical master plots (Fig. 3). The thermal decomposition mechanism of the compound was evaluated by comparing the experimentally derived master plots with their theoretical counterparts [50,51]. To further validate the mechanism, master plots of different kinetic functions versus α were generated from decomposition data collected at multiple heating rates under an nitrogen atmosphere. The comparison confirmed that the decomposition stage of the compound corresponds to the F3[52] master curve. Assuming the F3 theoretical model, the logarithm of the pre-exponential factor (ln A) for the decomposition stage was determined from the correlation coefficient of the plots of $0.5[(1-\alpha)^{-2}-1]$ against E_a $p(u)/\beta R$, yielding a value of 22.08 (Fig. 3). The results indicate a strong consistency between the value of *A* obtained from the above equation and that calculated using equation (4). Accordingly, the kinetic expression describing the non-isothermal decomposition of BBFPPO can be represented as:

$$\beta\frac{d\alpha}{dT} = 3.88\times10^{9}\times exp\left(-\frac{107340}{RT}\right)(1-\alpha)^{3} \quad \text{.....(4)}$$

Here, $(1-\alpha)^3$ corresponds to the differential form of the reaction-order model. For the non-isothermal decomposition of BBFPPO, the F3 model was found to provide the best fit across all three heating rates.

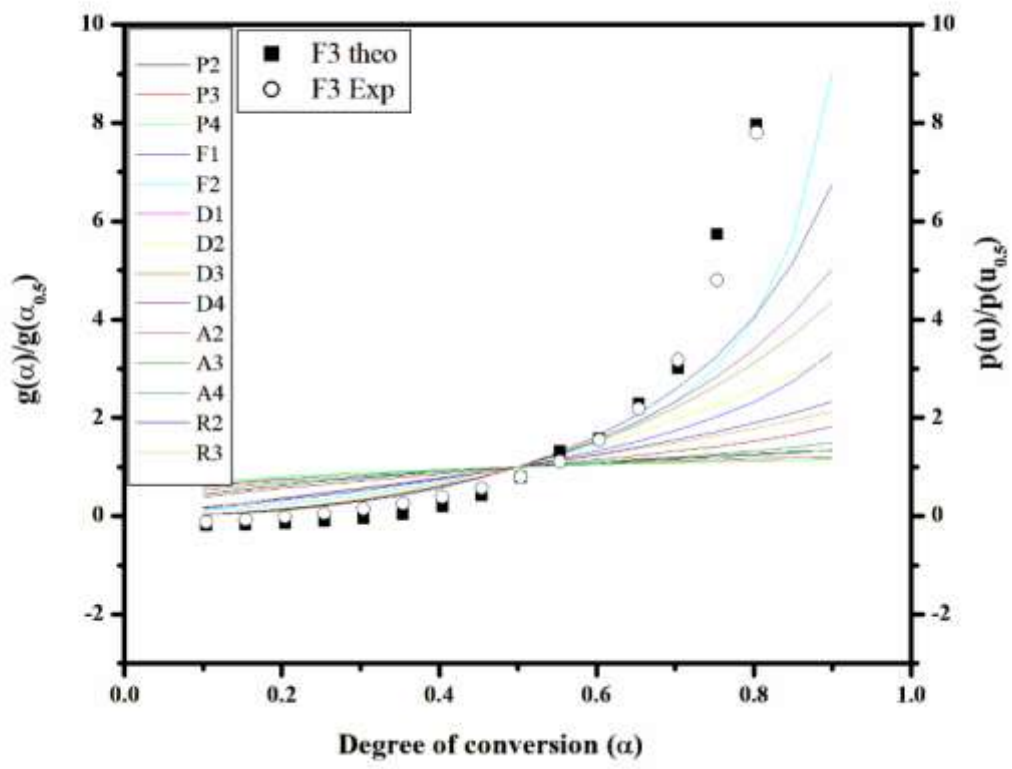

Fig 3. Plot of $g(\alpha)/g(\alpha_{0.5})$ and $p(u)/p(u_{0.5})$ versus degree of conversion (a) for BBFPPO

3.4 Thermodynamic parameters

Thermodynamic parameters of the compound were evaluated using equations [44], with the results are summarized in **Table 5.**. The negative entropy value, together with the positive Gibbs free energy, suggests that the decomposition is an endothermic process, requiring heat absorption during the compound's breakdown. A detailed summary of the thermal decomposition of BBFPPO under non-isothermal conditions in a nitrogen atmosphere is provided in **Table 6**.

REDVET - Revista electrónica de Veterinaria - ISSN 1695-7504
Vol 25, No. 1 (2024)
http://www.veterinaria.org
Article Received: 21/04/2023 Revised: 12/05/2023 Accepted: 01/06/2024

Table 5. Thermodynamic parameters of BFPPO under non-isothermal condition (DTG peak temperature)

β °C/min	Temperature K	lnA (A/min)	E_a kJ/mol	ΔS J/Kmol	ΔH kJ/mol	ΔG kJ/mol
10	623.0					
15	634.5	16.17	90.38	-125.01	85.11	164.43
20	646.0					

Table 6. Summary of thermal decomposition of BFPPO in the nitrogen under non-isothermal condition.

	Friedman	KAS	FWO
Isoconventional method E_a kJ/mol	107.34±3.4	100.98 ±3.3	105.00 ±3.3
Kinetic model g(α)	$0.5[(1-\alpha)^{-2}-1]$ (F3)		
Invariant kinetic parameters	E_a kJ/mol	100.19	
	lnA/min	22.08	

4. CONCLUSIONS

The compound undergoes a single-step decomposition process accompanied by heat absorption. The mechanism corresponds to the F3 model. It displays relatively low thermal stability, with the activation energy estimated through model-free approaches showing good agreement with the values obtained from thermodynamic analysis. The negative entropy value suggests that the decomposition leads to a more ordered system, while the positive Gibbs free energy confirms that the process is endothermic and non-spontaneous. These findings are in line with the results derived from TG-DTG/DTA analyses.

Acknowledgements

The Authors pay sincere gratitude to Department of Chemistry, Annamalai university for IR spectrum and thermal analyzer, STA 7200, Hitachi HTG, Vignan University,Andhra Pradesh for TG, DTA and DTG analyses.

References

[1] Kumar KA, Jayaroopa P (2013) Isoxazoles: molecules with potential medicinal properties. Int J Pharm Chem Biol Sci 3: 294-304.
[2] Perumal V, Adiraj M, Pandiyan P (2001) Synthesis, analgesic and anti inflammatory evaluation of substituted 4-piperidones. Indian drugs-bombay 38: 156-159.
[3] Hagenbach RE, Gysin H (1952) Über einige heterozyklische Thiosemicarbazone. Experientia 8: 184-185. https://doi.org/10.1007/BF02173735
[4] Katritzky AR, Fan W (1990) The chemistry of benzotriazole: A novel and versatile synthesis of 1-alkyl-,1-aryl-, 1-(alkylamino)-, or 1-amido-substituted and of 1,2,6-trisubstituted piperidines from glutaraldehyde and primary amines or monosubstituted hydrazines. The Journal of Organic Chemistry 55(10): 3205-3209. https://doi.org/10.1021/jo00297a041
[5] Ganellin CR, Spickett RGW (1965) Compounds affecting the central nervous system. I. 4-Piperidones and related compounds. Journal of Medicinal Chemistry 8(5): 619-625. https://doi.org/10.1021/jm00329a015
[6] Agarwal OP (2002) Chemistry of organic natural products. Goel Publishing House (Vol. 2): Meerut, India.
[7] Finar IL (1975) Organic chemistry London. England ELBS Vol. 2: pp. 651-660.
[8] Wagstaff AJ, Cheer SM, Matheson AJ, Ormrod D, Goa KL (2002) Paroxetine: an update of its use in psychiatric disorders in adults. Drugs *62*(4): 655-703. https://doi.org/10.2165/00003495-200262040-00010
[9] Abdel-Fatah SM, Díaz-Sánchez M, Díaz-García D (2020) Nanostructured metal oxides prepared from Schiff base metal complexes: Study of the catalytic activity in selective oxidation and C–C coupling reactions. Journal of Inorganic and Organometallic Polymers and Materials 30(5): 1293-1305. https://doi.org/10.1007/s10904-019-01269-y
[10] Kong Q, Zhang J, Zhang K, Wang S, He M, Guo Y, Gu J (2025) Recyclable side-chain azobenzene-based semicrystalline polymer films with outstanding intrinsic thermal conductivity and photoresponsive actuation. Angewandte Chemie 137(37): Advance online publication. https://doi.org/10.1002/ange.202512721
[11] Moody CJ (2004) Addition reactions of ROPHy/SOPHy oxime ethers: Asymmetric synthesis of nitrogen-containing compounds. Chemical Communications (12): 1341-1351.
[12] Escolano C, Amat M, Bosch J (2006) Chiral Oxazolopiperidone Lactams: Versatile Intermediates for the Enantioselective Synthesis of Piperidine-Containing Natural Products. Chem. - Eur. J 12: 8198-8207.
[13] Remuson R, Gelas-Mialhe Y (2008) A Convenient Access to the Piperidine Ring by Cyclization of Allylsilyl Substituted N-cyliminium and Iminium Ions: Application to the Synthesis of Piperidine Alkaloids. Mini-Reviews in Organic Chemistry 5(3): 193-208. https://doi.org/10.2174/157019308785161701

[14] Amat M, Llor N, Griera R, Pérez M, Bosch J (2011) Enantioselective synthesis of alkaloids from phenylglycinol-derived lactams. Natural Product Communications 6(4). https://doi.org/10.1177/1934578X1100600412
[15] Seki H, Georg GI (2014) 2,3-Dihydropyridin-4(1H)-ones and 3-aminocyclohex-2-enones: Synthesis, functionalization, and applications to alkaloid synthesis. Synlett *25*(18): 2536-2557. https://doi.org/10.1055/s-0034-1378529
[16] Kandepedu N, Abrunhosa-Thomas I, Troin Y (2017) Stereoselective strategies for the construction of polysubstituted piperidinic compounds and their applications in natural products synthesis. Organic Chemistry Frontiers 4(8): 1655-1704. https://doi.org/10.1039/C7QO00262A
[17] Zhang W, Ai J, Shi D, Peng X, Ji Y, Liu J, Geng M, Li Y (2014) Discovery of Novel c-Met Inhibitors Bearing a 3-Carboxyl Piperidin-2-one Scaffold. Molecules 19(2): 2655-2673. https://doi.org/10.3390/molecules19022655
[18] Li L, Chen M, Jiang FC (2016) Design, synthesis, and evaluation of 2-piperidone derivatives for the inhibition of β-amyloid aggregation and inflammation mediated neurotoxicity. Bioorganic & Medicinal Chemistry 24(8): 1853-1865. https://doi.org/10.1016/j.bmc.2016.03.010
[19] Climent MJ, Corma A, Iborra S (2012) Homogeneous and heterogeneous catalysts for multicomponent reactions. RSC Advances 2(1): 16-58. https://doi.org/10.1039/C1RA00807B
[20] Takasu K, Shindoh N, Tokuyama H, Ihara M (2006) Catalytic imino Diels-Alder reaction by triflic imide and its application to one-pot synthesis from three components. Tetrahedron 62(51): 11900-11907. https://doi.org/10.1016/j.tet.2006.09.092
[21] Sales M, Charette AB (2005) A Diels-Alder Approach to the Stereoselective Synthesis of 2, 3, 5, 6-Tetra-and 2, 3, 4, 5, 6-Pentasubstituted Piperidines. Organic Letters 7(26): 5773-5776. https://doi.org/10.1021/ol052436v
[22] Carballo RM, Ramírez MA, Rodríguez ML, Martín VS, Padrón JI (2006) Iron (III)-promoted aza-Prins-cyclization: direct synthesis of six-membered azacycles. Organic Letters *8*(17): 3837-3840. https://doi.org/10.1021/ol061448t
[23] Dobbs AP, Guesné SJ (2005) Rapid access to trans-2, 6-disubstituted piperidines: expedient total syntheses of (-)-solenopsin A and (+)-epi-dihydropinidine. Synlett (13): 2101-2103. https://doi.org/10.1055/s-2005-871956
[24] Fustero S, Jiménez D, Moscardó J, Catalan S, Del Pozo C (2007) Enantioselective organocatalytic intramolecular aza-Michael reaction: a concise synthesis of (+)-sedamine,(+)-allosedamine and (+)-coniine. Organic letters 9(25): 5283-5286. https://doi.org/10.1021/ol702447y
[25] Davis FA, Chao B, Rao A (2001) Intramolecular Mannich reaction in the asymmetric synthesis of polysubstituted piperidines: concise synthesis of the dendrobate alkaloid (+)-241D and its C-4 epimer. Organic Letters 3(20): 3169-3171. https://doi.org/10.1021/ol0164839
[26] Venkatesan P, Maruthavanan T (2015) Stereochemical effect on biological activities of new series of piperidin-4-one derivatives. Natural Product Research 29(22): 2092-2096. https://doi.org/10.1080/14786419.2015.1009456
[27] Casy AF, Coates JE, Rostron C (1976) Reversed ester analogues of pethidine: isomeric 4-acetoxy-1, 2, 6-trimethyl-4-phenyrpiperidines. Journal of Pharmacy and Pharmacology 28(2): 106-110. https://doi.org/10.1111/j.2042-7158.1976.tb04107.x
[28] Vijayakumar V, Sundaravadivelu M, Perumal S (2001) NMR and IR spectroscopic study of mono- bi- and tricyclic piperidone systems. Magnetic Resonance in Chemistry 39(2): 101-104. https://doi.org/10.1002/1097-458X(200102)39:2%3C101::AID-MRC797%3E3.0.CO;2-F
[29] Rajesh K, Reddy BP, Vijayakumar V (2012) Ultrasound-promoted synthesis of novel bipodal and tripodalpiperidin-4-ones and silica chloride mediated conversion to its piperidin-4-ols: Synthesis and structural confinements. Ultrasonics Sonochemistry 19(3): 522-531. https://doi.org/10.1016/j.ultsonch.2011.10.018
[30] Suresh T, Sarveswari S, Vijayakumar V, Iniyavan P, Srikanth A, Jasinski JP (2015) Synthesis, spectral characterization and DFT analysis for the validation of 2, 6 diaryl-piperidin-4-ones as potential sunscreens and UV filters. Journal of Molecular Structure 1099: 560-566. https://doi.org/10.1016/j.molstruc.2015.07.011
[31] Ahamed A, Arif I A, Mateen M, Kumar RS, Idhayadhulla A (2018) Antimicrobial, anticoagulant, and cytotoxic evaluation of multidrug resistance of new 1, 4-dihydropyridine derivatives. Saudi Journal of Biological Sciences 25(6): 1227-1235. https://doi.org/10.1016/j.sjbs.2018.03.001
[32] Subha Nandhini M, Vijayakumar V, Mostad A, Sundaravadivelu M, Natarajan S (2003) Ethyl 4-oxo-2, 6-diphenyl-4-piperidine-3-carboxylate. Structure Reports 59(11): 1672-1674. https://doi.org/10.1107/S1600536803021792
[33] Vijayakumar V, Rajesh K, Suresh J, Narasimhamurthy T, Lakshman PN (2010) 1, 1′-(p-Phenylenedimethylene) dipiperidin-4-one. Structure Reports 66(1): 170. https://doi.org/10.1107/S1600536809052908.
[34] Rajarajan G, Dhineshkumar E, Amala S, Thanikachalam V, Selvanayagam S, Sridhar B (2020) Synthesis, spectral characterization (FT-IR, NMR, XRD) and computational studies of chloroacetyl chloride incorporated 3t-butyl-2r, 6c-diphenyl/di (thiophen-2-yl) piperidin-4-ones. Journal of Molecular Structure 1200: 127076. https://doi.org/10.1016/j.molstruc.2019.127076
[35] Rajesh K, Vijayakumar V, Sarveswari S, Narasimhamurthy T, Tiekink ER (2010) 1-{3-[(4-Oxopiperidin-1-yl) carbonyl] benzoyl} piperidin-4-one. Structure Reports 66(8): 1988. https://doi.org/10.1107/s1600536810026681.

[36] Nelson KM, Dahlin JL, Bisson J, Graham J, Pauli GF, Walters MA (2017) The essential medicinal chemistry of curcumin: miniperspective. Journal of medicinal chemistry 60(5): 1620-1637.https://doi.org/10.1021/acs.jmedchem.6b00975
[37] Dimmock JR, Jha A, Zello GA, Quail JW, Oloo EO, Nienaber KH, Stables JP (2002) Cytotoxic N-[4-(3-aryl-3-oxo-1-propenyl) phenylcarbonyl]-3, 5-bis (phenylmethylene)-4-piperidones and related compounds. European journal of medicinal chemistry 37(12):961-972.https://doi.org/10.1016/S0223-5234(02)01414-9
[38] Martínez-Cifuentes M, Weiss-López B, Araya-Maturana R (2016) A computational study of structure and reactivity of N-substitued-4-piperidones curcumin analogues and their radical anions. Molecules 21:1-10. https://doi.org/10.3390/molecules21121658
[39] Reed AE, Curtiss LA, Weinhold F (1988) Intermolecular interactions from a natural bond orbital, donor-acceptor viewpoint. Chemical Reviews 88: 899-926. https://doi.org/10.1021/cr00088a005
[40] Noller CR, Balliah V (1948) Preparation of some piperidine derivatives by the Mannich reaction. Journal of American chemical society 70: 3853-3855.
[41] Nagendra Babu K, Vallal Perumal G, Rajarajan G, Manikandan G, Thanikachalam V (2023) Thermal vaporization of (E)-methyl-2-hydroxy-5-(phenyldiazenyl)benzoate under non-isothermal condition in air atmosphere. Gravida Review J 9 (11): 550-573.
[42] Friedman HL (1963) Kinetics of thermal degradation of char-forming plastics from thermogravimetry. Application to a phenolic plastic. J Polym Sci Part C: Polym Lett 6: 183-195. https://doi.org/10.1002/polc.5070060121
[43] Flynn JH, Wall LA (1966) General treatment of the thermogravimetry of Polymers. J Res Natl Bur Stand Sect A 70: 487-523. https://doi.org/10.6028/jres.070A.043
[44] Akahira T, Sunose T (1971) Joint convention of four electrical institutes. Res Rep Chiba Inst Technol 16: 22-31.
[45] Coats AW Redfern JP (1964) Kinetic parameters from thermogravimetric data. Nature 201: 68-69. https://doi.org/10.1038/201068a0
[46] Lesnikovich AI, Levchik SV (1983) A method of finding invariant values of kinetic parameters. Journal of Thermal Analysis 27: 89-93. https://doi.org/10.1007/BF01907324
[47] Lesnikovich AI, Levchik SV (1985) Isoparametric kinetic relations for chemical transformations in condensed substances (Analytical Survey). J Therm Anal 30: 237-262. https://doi.org/10.1007/bf02128134
[48] Vyazovkin S, Lesnikovich AI (1988) Estimation of the pre-exponential factor in the isoconversional calculation of effective kinetic parameters. Thermochim Acta 128: 297-300. https://doi.org/10.1016/0040-6031(88)85372-3.
[49] Cai J, Li LS (2009) Kinetic Analysis of wheat straw pyrolysis using isoconversional methods. Journal of Thermal Analysis Calorimetric 98: 325-330. https://doi.org/10.1007/s10973-009-0325-8
[50] Malek J **(1992)** The Kinetic analysis of non-isothermal data. Thermochimica Acta 200: 257-269. https://doi.org/10.1016/0040-6031(92)85118-F
[51] Sbirrazzuoli N, Vecchio S, Catalani A (2005) Isoconversional kinetic study of alachlor and metolachlor vaporization by thermal analysis. International Journal of Chemical Kinetics 37:74-80. https://doi.org/10.1002/kin.20054
[52] Busto Y, Tack FMG, Peralta L M, Cabrera X, Arteaga-Perez LE (2013) An Investigation on the modelling of kinetics of thermal decomposition of hazardous mercury wastes. Journal of Hazardous Materials 260: 358-367. https://doi.org/10.1016/j.jhazmat.2013.05.045